Available online at www.sciencedirect.com
ScienceDirect
Talanta 74 (2008) 1337–1343
Talanta
www.elsevier.com/locate/talanta

In situ electrodeposited nanoparticles for facilitating electron transfer across self-assembled monolayers in biosensor design

Dan Du [a,*], Jiawang Ding [a], Jie Cai [b], Jianming Zhang [a], Li Liu [a]

[a] *Key Laboratory of Pesticide and Chemical Biology of Ministry of Education, College of Chemistry, Central China Normal University, Wuhan 430079, PR China*
[b] *The Technology Center of Wuhan Iron & Steel Company, Wuhan 430080, PR China*

Received 23 May 2007; received in revised form 6 September 2007; accepted 6 September 2007
Available online 14 September 2007

Abstract

Gold nanoparticles (AuNPs) were synthesized *in situ* and electrodeposited onto Au substrate. The AuNPs modified interface facilitates electron transfer across self-assembled monolayers (SAMs) of 11-mercaptoundecanoic acid (MUA). After activation of surface carboxyl groups with 1-ethyl-3-(3-dimethylaminopropyl) carbodiimide and *N*-hydroxysuccinimide, the interface displayed good stability for immobilization of biomolecules. These modification processes were characterized by contact angle measurement, cyclic voltammetry and electrochemical impedance spectra. The immobilized acetylcholinesterase (AChE), as a model, showed excellent activity to its substrate, leading to a stable AChE biosensor. Under the optimal experimental conditions, the inhibition of malathion on AChE biosensor was proportional to its concentration in two ranges, from 0.001 to 0.1 μg mL^{-1} and from 0.1 to 25 μg mL^{-1}, with detection limit of 0.001 μg mL^{-1}. The simple method showed good reproducibility and acceptable stability, which had potential application in biosensor design.

Keywords: Electrodeposition; Gold nanoparticles; Self-assembled monolayers; Organophosphate pesticides; Biosensor

1. Introduction

Enzymes are the most powerful molecular recognition elements in biosensing, since the sensing signal can be amplified millions of times through enzymatic reactions [1]. This signal amplification enables the design of highly sensitive biosensing systems. Amperometric enzymatic biosensors have been considered to be the most suitable for biochemical analysis due to their good selectivity, sensitivity, rapid response, miniature size, and reproducible results [2]. A combination of enzymatic reactions with the electrochemical method allows developing different enzyme-based electrochemical biosensors for sensitive and rapid determination of environmental analysis [3]. Among these, amperometric acetylcholinesterase (AChE) biosensors have shown satisfactory results for pesticides analysis based on their inhibition on AChE [4–6], in which the enzymatic activity is employed as an indicator of quantitative measurement of pesticides.

A significant challenge to develop sensitive and stable biosensors comes from the effective immobilization of enzyme to solid electrode surface [7,8]. Generally, direct adsorption of enzyme onto bare gold surface can frequently result in their denaturation and the loss of bioactivity [9]. Self-assembled monolayers (SAMs) of alkanethiols on gold substrate provide an easy method to create well-defined surfaces with controllable chemical functionality, and partly as a functionalized structure for further modification of the surface [10]. This interface has been used to anchor different functional groups in biosensors design [11,12]. For example, when the terminal group of thiolate SAMs is a carboxylic group, the modified gold surface combining the unique properties of SAMs with the carbodiimide chemistry offers a further functionalization with biomolecules, such as proteins [13,14], DNA [15], and antibody [16].

The SAMs serves partly as a barrier to prevent proteins and other ligands from coming into contact with the metal. The stable, close-packed, and well-ordered SAMs on gold electrodes usually display a very low fraction of defects [17,18]. They are strongly resistant to ion penetration, and may therefore impede the electron transfer between the electrode surface and the electroactive species in solution. To circumvent the

* Corresponding author. Tel.: +86 27 67867953.
E-mail address: dudan@mail.ccnu.edu.cn (D. Du).

0039-9140/$ – see front matter © 2007 Elsevier B.V. All rights reserved.
doi:10.1016/j.talanta.2007.09.003

drawbacks of electron transfer, a possible route consists in incorporating metal nanoparticles. Metal nanoparticles provide three important functions for electroanalysis: the roughening of the conductive sensing interface, catalytic properties, and conductivity properties [19]. Among several nano-materials, gold nanoparticles (AuNPs) have been widely used for preparation of electrochemical biosensors [20,21]. Generally, AuNPs could be easily fabricated by standard methods [22] or electrochemical technologies [23]. Compared with traditional process, electrochemical deposition is simple, the performance conditions are moderate, and it is suitable for selective deposition of films with controllable thickness [24], which provides an easy and rapid alternative for the preparation of AuNPs modified electrodes in a short time [25].

The present work is motivated by very promising applications of AuNPs facilitating electron transfer. At a constant applied potential, AuNPs were synthesized *in situ* and electrodeposited onto gold electrode surface. SAMs of 11-mercaptoundecanoic acids were then formed onto the resulting surface. After activation of surface carboxyl groups with 1-ethyl-3-(3-dimethylaminopropyl) carbodiimide and *N*-hydroxysuccinimide, the interface possessing good stability is suitable for facile immobilization of enzyme, leading to a stable AChE biosensor (Scheme 1) for quantitative measure of organophosphate pesticide. The immobilized AChE, as a model showed excellent activity to its substrate. In order to estimate the properties of the interface, several methods such as cyclic voltammetric scan and electrochemical impedance have been used to characterize and optimize the deposition conditions.

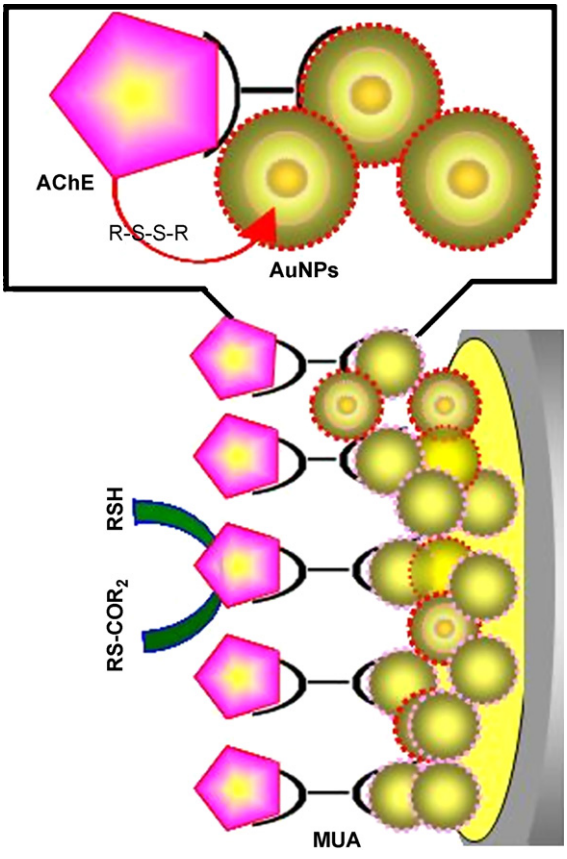

Scheme 1. Principle of AuNPs served as mediator for electron transfer across SAMs for AChE biosensor design.

2. Experimental

2.1. Reagents

Acetylthiocholine chloride (ATCl), Acetylcholinesterase (Type C3389, 500 U mg^{-1} from electric eel) and 11-mercaptoundecanoic acid (MUA) were purchased from Sigma–Aldrich (St. Louis, USA) and used as received. 1-ethyl-3-(3-dimethylaminopropyl) carbodiimide (EDC), *N*-hydroxysuccinimide (NHS) were obtained from Aldrich Chemical Company Inc. $HAuCl_4{\cdot}4H_2O$ (Au > 48%) was obtained from TreeChem.co (China). Malathion was obtained from AccuStandard (USA). $Fe(CN)_6^{4-/3-}$, phosphate buffer solution (PBS, pH 7.0) and other reagents used were of analytical reagent grade. Aqueous solution was prepared with double distilled water.

2.2. Instruments

Cyclic voltammetric measurements were performed on a Bio-analytical System (BAS, cv-50w, USA) with a conventional three-electrode system comprising platinum wire as auxiliary electrode, Ag/AgCl (3 M NaCl) as reference. AChE coupled to MUA-AuNPs modified gold electrode (AChE-MUA-AuNPs/Au) was used as working electrode. The ac impedance experiment was carried out in 5 mM $Fe(CN)_6^{4-/3-}$ with frequencies ranging from 100 kHz to 0.1 Hz with a CHI 660C electrochemical workstation. The static water contact angle was measured at 25 °C by a contact angle system OCA 20 (Dataphysics, Germany). Measurements were repeated on at least four drops.

2.3. Preparation of AChE-MUA-AuNPs/Au

Gold disk electrode with a polypropylene body (1.0 mm in diameter) was used for the electrochemical measurement. Before modification, the gold electrode was abraded with fine SiC paper, lightly polished with 0.05 μm alumina (Buhler), followed by sonication in ethanol and double distilled water for 10 min, respectively. The electrochemical pretreatment was performed in a BAS cell by cycling from a potential of −0.1 to +1.25 V versus Ag/AgCl in 0.1 M H_2SO_4 solution until a stable and reproducible gold oxidation peak at +1.1 V versus Ag/AgCl was obtained [26].

For electrochemical deposition, Time-Base mode was used. Briefly, a clean gold electrode was immersed in 0.1% $HAuCl_4{\cdot}4H_2O$ and an initial potential of +0.15 V was applied on the electrode. The resulting AuNPs-deposited gold electrode (AuNPs/Au) was immersed in 1 mM MUA for 3 h to prepare MUA monolayer modified AuNPs/Au (MUA-AuNPs/Au). After activation using 0.2 M EDC and 0.05 M NHS for 30 min, the carboxyl groups were activated to form reactive *N*-hydroxysuccinimide esters. Then 3.0 μL AChE solution

(100 mU) was dropped and dried in air at room temperature for another 2 h. After washing carefully with PBS to remove non-specifically adsorbed enzyme, the AChE-MUA-AuNPs/Au was obtained.

2.4. Measurement procedure

For measurement of malathion, the pretreated AChE-MUA-AuNPs/Au was first immersed in standard malathion solutions with different concentration for 12 min, and then transferred to the electrochemical cell of 1.0 mL pH 7.0 PBS containing 0.3 mM ATCl to study the electrochemical response by cyclic voltammetry (CV). The inhibition of malathion was calculated as follows:

$$\text{Inhibition}\,(\%) = 100 \times \frac{i_{\text{P,control}} - i_{\text{P,exp}}}{i_{\text{P,control}}}$$

where $i_{\text{P,control}}$ is the peak current of ATCl on the AChE-MUA-AuNPs/Au, $i_{\text{P,exp}}$ is the peak current of ATCl on the AChE-MUA-AuNPs/Au with malathion inhibition.

3. Results and discussion

3.1. Electrodeposition of AuNPs on gold electrode

Cyclic voltammetric measurement for gold electrodes in 0.1% $HAuCl_4{\cdot}4H_2O$ solution revealed that reduction of $AuCl_4^-$ occurred at a peak potential of +0.18 V (inset in Fig. 1). Thus, an initial potential of +0.15 V was selected for deposition of AuNPs. The obtained AuNPs/Au showed two reduction peaks differing in the reduction potential (Fig. 1a), while only one reduction peak was observed at bare gold electrode (Fig. 1b). The single reduction peak at +0.88 V (versus Ag/AgCl 3 M NaCl) was attributed to the reduction of gold surface oxide [27]. The two-reduction peak was due to the different reduction abilities of the oxidized AuNPs and the oxidized plane gold surface [28]. It is also obvious that the cathodic peak current of the AuNPs/Au was higher than that of bare gold electrode, indicating that AuNPs modified gold electrode had a larger surface area. The real surface areas of AuNPs/Au and bare gold were determined by integrating the reduction peak area of oxidized gold layer formed by CV scans from −0.2 to +1.6 V in 0.5 M H_2SO_4 [29,30] and thus the roughness factor could be estimated. The real surface area of AuNPs/Au by electrodeposition was calculated to reach 0.0564 cm^2, while the real surface area of bare gold electrode was 0.0357 cm^2. The roughness factor increased from 1.14 of bare gold electrode to 1.52 of AuNPs/Au with electrodeposition time of 120 s. Nanoparticles with deposition time of 120 s have average particle sizes in the range of 20–40 nm [26].

It has been reported that by varying the deposition time at a constant applied potential, AuNPs with different sizes and densities could be deposited onto gold electrode and the big-size gold clusters led to a much rougher electrode surface [26]. When the deposition time reaches to 180 s, big size gold clusters may form on the gold electrode surface. This packed clusters on the electrode surface would somewhat block the electron transfer. Thus, 120 s was chosen as deposition time.

3.2. Preparation of the MUA-AuNPs/Au monolayer

$Fe(CN)_6^{4-/3-}$ redox system as one of the most extensively studied redox couples in electrochemistry was used to confirm the properties and changes of deposited surface. Theoretically, the electron transfer rate or electron transfer resistance of electroactive probe on electrode surface was related to the surface properties. As seen from Fig. 2, when MUA was assembled directly on Au electrode (MUA/Au), the CV curves of $Fe(CN)_6^{4-/3-}$ probe on MUA/Au resulted in a sharp decrease in peak currents with the increase of assembling time from 1

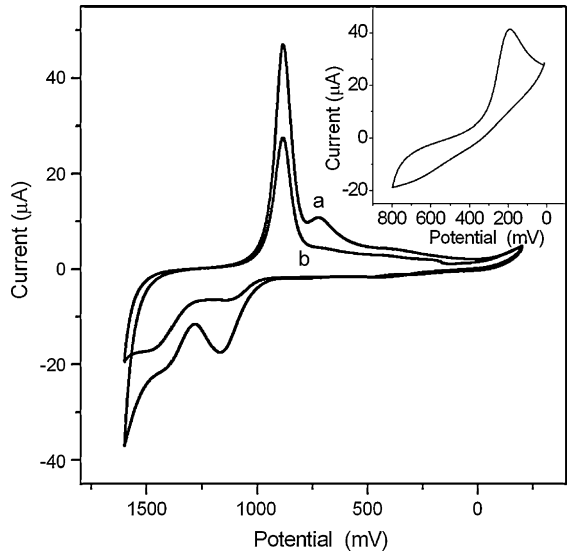

Fig. 1. Cyclic voltammograms of AuNPs/Au (a) and bare Au (b) in 0.5 M H_2SO_4. Inset: cyclic voltammograms of 0.1% $HAuCl_4{\cdot}4H_2O$ reduction.

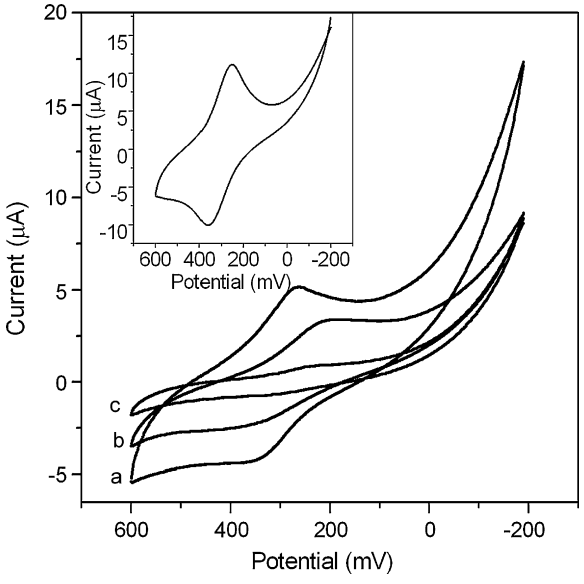

Fig. 2. Cyclic voltammograms of $Fe(CN)_6^{4-/3-}$ at MUA/Au with MUA assembling time of 1 h (a), 2 h (b) and 3 h (c). Inset: cyclic voltammogram of $Fe(CN)_6^{4-/3-}$ at MUA-AuNPs/Au with MUA assembling time of 3 h.

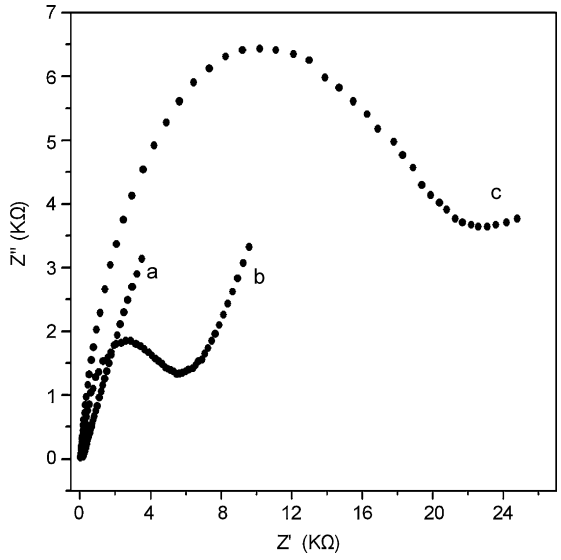

Fig. 3. Electrochemical impedance spectra of bare Au electrode (a), MUA-AuNPs/Au (b) and MUA/Au (c) in 5 mM $Fe(CN)_6^{4-/3-}$.

to 3 h. The encumbrance of the electron transfer was due to the negatively charged surface of MUA modified electrode, which blocked $Fe(CN)_6^{3-/4-}$ go through the MUA film to exchange the electron with electrode. No obvious redox peaks were observed for further assembling, indicating a close-packed and well-ordered SAMs was formed with 3 h. However, it was worthwhile mentioning that the CV of $Fe(CN)_6^{4-/3-}$ probe on MUA-AuNPs/Au displayed a significant change. A couple of redox peaks with much larger peak currents were observed (inset in Fig. 2). This phenomenon was due to the deposited AuNPs, which improved conductive sensing interface and thus circumvented the drawbacks of electron transfer across the MUA interface. The same result was also obtained in the following experiment. Therefore, MUA-AuNPs/Au was selected as support surface for biosensor design.

Furthermore, the MUA-AuNPs/Au displayed a reduction peak at −1.10 V in 0.5 M KOH. This peak was attributed to the reductive desorption of the thiolated compounds bound to gold [31,32], indicating the presence of the MUA molecule on Au surface. The reaction for reductive desorption of thiolated compounds is: $Au\text{-}SR + e^- \rightarrow Au + RS^-$ [33]. From the integration of the reductive desorption peak, the surface coverage, Γ ($\Gamma = Q/nFA$ and $A = 0.0564\,cm^2$), was calculated to be 7.63×10^{-10} mol/cm^2, which means that each molecules occupies a surface area of 21.8 A^2 on average. Following Dubois and Zegarski [34], simple alkanethiols require an area of about 21.4 A^2 if deposited as densely packed SAMs on Au. These results indicated a densely packed MUA monolayer on AuNPs modified electrode.

3.3. ac impedance measurements

Fig. 3 showed the results of electrochemical impedance spectra (EIS) on modified electrodes. The electron transfer resistances of $Fe(CN)_6^{4-/3-}$ at bare gold electrode (curve a), MUA-AuNPs/Au (curve b), and MUA/Au (curve c) were 26, 6352 and 23,145 Ω, respectively. The significant change occurred at MUA/Au, indicating that MUA monolayer introduced a barrier to electrochemical process. However, an obvious decrease in charge-transfer resistance at MUA-AuNPs/Au was clearly observed. This change might be related to electrodeposited AuNPs, which decreased the impedance of interface and resulted in the electron exchange of $Fe(CN)_6^{4-/3-}$ across the MUA SAMs. This result was in accordance with the electrochemical probe assays as detailed above.

3.4. Contact angle measurements

Contact angle measurements were carried out to confirm the properties and changes of deposited surface. As shown in Fig. 4, the bare Au and MUA/Au gave the contact angles of 72.1° and 61.4°, respectively. The MUA surface showed comparatively high hydrophilicity, which was not surprising since the terminal carboxylate group was highly polar [35]. For MUA-AuNPs/Au, the contact angle decreased to be 47.5° (Fig. 4C). The decrease in contact angle was due to roughening of the conductive sensing interface, which had a large real surface area for MUA assembling and more terminal carboxylate groups. Thus, the electrodeposited AuNPs not only improved the electro transfer, but also increased the surface hydrophilicity. This interface was suitable for facile immobilization of biomolecules.

3.5. Cyclic voltammetric behavior of AChE-MUA-AuNPs/Au

AChE, as a model, was immobilized onto MUA-AuNPs/Au surface after activation of carboxy groups in MUA molecule. As shown in Fig. 5, no peak was observed at MUA-AuNPs/Au (curve a) and AChE-MUA-AuNPs/Au (curve b) in pH 7.0 PBS. When 0.3 mM ATCl was added into PBS, the AChE-MUA-AuNPs/Au showed an irreversible oxidation peak at 859 mV (curve e), while no detectable signal was observed at MUA-AuNPs/Au (curve c). Obviously this peak

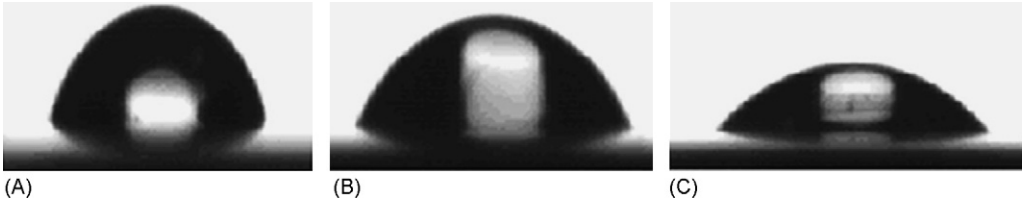

Fig. 4. Contact angle graphs of bare Au substrate (A), MUA/Au (B) and MUA-AuNPs/Au (C).

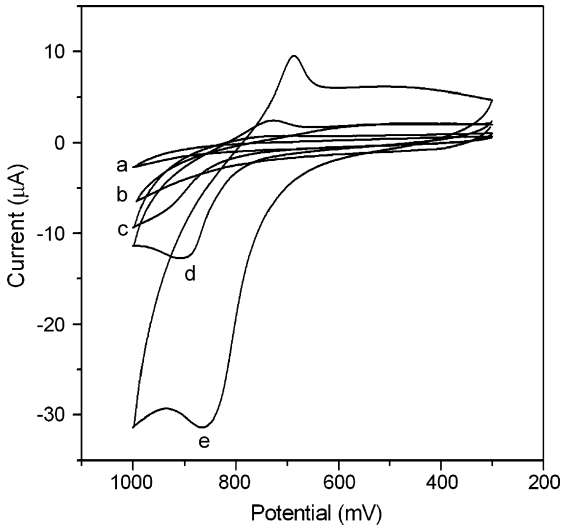

Fig. 5. Cyclic voltammograms of MUA-AuNPs/Au (a and c), AChE-MUA/Au (b) and AChE-MUA-AuNPs/Au (b and e). Supporting electrolyte: pH 7.0 PBS (a and b) and pH 7.0 PBS containing 0.3 mM ATCl (c–e).

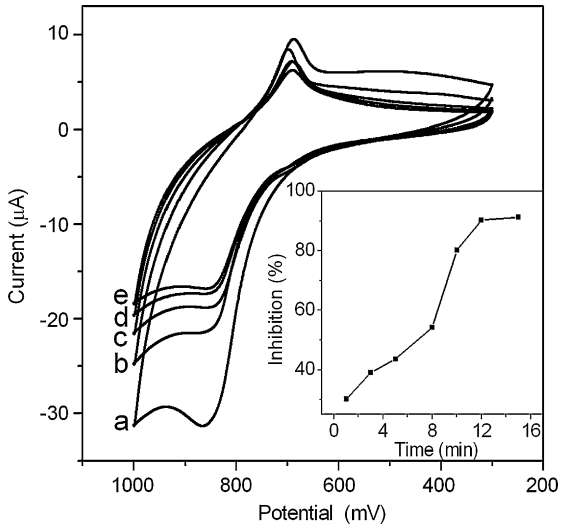

Fig. 6. Cyclic voltammograms of AChE-MUA-AuNPs/Au in pH 7.0 PBS containing 0.3 mM ATCl after inhibition with 2.0 μg mL^{-1} malathion for 1 min (a), 3 min (b), 5 min (c), 8 min (d) and 10 min (e). Inset: dependence of malathion inhibition curve on inhibition time.

came from the oxidation of thiocholine, hydrolysis product of ATCl, which was catalyzed by immobilized AChE. The reaction between AChE-MUA-AuNPs/Au electrode and ATCl substrate was a CE coupled reaction, including a chemical reaction: $EH + RS\text{-}COR_2 \rightarrow RSH + E\text{-}COR_2$ and an electrode reaction: $RSH - 2e^- \rightarrow RSSR + 2H^+$. It was interesting to compare the current responses at AChE-MUA/Au and AChE-MUA-AuNPs/Au. The peak current of ATCl on AChE-MUA-AuNPs/Au was much higher and the peak potential shifted negatively compared to those on AChE-MUA/Au electrode without AuNPs (curves d and e). These phenomena were attributed to the presence of electrodeposited AuNPs, which possessed inherent conductive properties and thus provided a conductive pathway to electron transfer and promoted electron transfer reactions at a lower potential. The produced current on AChE-MUA-AuNPs/Au reflected enzymatic activity, which could be used for organophosphate pesticides analysis involved in the inhibition action [36,37].

3.6. Effect of incubation time on response of AChE-MUA-AuNPs/Au

Upon AChE-MUA-AuNPs/Au was immersed in the standard solution of malathion at a known concentration for different time, the produced current of ATCl on AChE-MUA-AuNPs/Au decreased drastically. The decrease in peak current was related to the increase of incubation time (Fig. 6). This was because malathion as one of the organophosphate pesticide involved in the inhibition action to AChE, thus reduced the enzymatic activity to its substrate. As seen from inset of Fig. 6, malathion displayed increasing inhibition to AChE with immersing time. When the immersing time was longer than 12 min the curve trended to a stable value, indicating the binding interaction with active target groups in enzyme could reach saturation. This change tendency of peak current reflected the alteration of enzymatic activity, which resulted in the change of the interactions with its substrate. However, the maximum value of inhibition of malathion was not 100%, which was likely to attribute to the binding equilibrium between pesticide and binding sites in enzyme.

3.7. Calibration curve

Due to the notable change in voltammetric signal of the AChE-MUA-AuNPs/Au, the simple method for determination of malathion was established. With increasing malathion concentrations the produced currents of ATCl on AChE-MUA-AuNPs/Au decreased. Under the optimal experimental conditions, the malathion inhibition on AChE-MUA-AuNPs/Au was proportional to the malathion concentrations in two ranges, from 0.001 to 0.1 μg mL^{-1} and from 0.1 to 25 μg mL^{-1}, The regression equation was $I\ (\%) = 11.53 + 59.68c$ and $I\ (\%) = 15.94 + 2.40c$, with the correlation coefficients of 0.9990 and 0.9969, respectively (Fig. 7). The detection limit was 0.001 μg mL^{-1}.

To further demonstrate the practicality of the proposed method, the recovery test was studied by adding different amounts of malathion into garlic samples. Results were summarized in Table 1. The recoveries were from 96.8 to 104.7 %. The results indicated that the proposed method can be used for direct analysis of relevant samples.

Table 1
Recovery studies of malathion in garlic samples

Samples	Concentrations		Recovery (%)
	Taken (μg mL^{-1})	Found (μg mL^{-1})	
1	0.010	0.0968	96.8
2	0.200	0.197	98.5
3	2.500	2.528	101.1
4	5.000	5.235	104.7

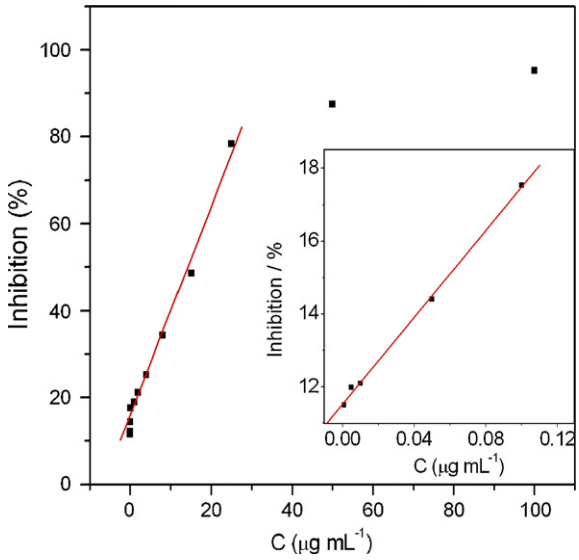

Fig. 7. Relationship between inhibition and concentration. Inset: linear relationship between inhibition and low concentration.

We are currently facing the disadvantage of the low selectivity of AChE because the degree of inhibition on AChE by organophosphate pesticide is almost the same. However, this does not necessarily compromise its value extended toward the preparation of other electrochemical sensors based on this mode. The ease of performance and the cost effectiveness of the system for malathion detection show the high potentiality in total amount of pesticide analysis. Regarding other possible interferences such the heavy metals, we can suppose that these inhibitors cannot interfere with the proposed biosensor because of its reversible inhibition on AChE.

3.8. Precision, reproducibility and stability of AChE-MUA-AuNPs/Au

The inter-assay precision was estimated by determining the response of 0.3 mM ATCl at six different electrodes, which were immersed in 0.1 μg mL^{-1} and 2.0 μg mL^{-1} malathion for 12 min, respectively. The coefficients of variation were calculated to be 2.4% and 3.1%, respectively, indicating acceptable fabrication reproducibility. The intra-assay precision of the sensors was evaluated by assaying one enzyme electrode for six replicate determinations, and the R.S.D. was 2.0% at the ATCl concentration of 0.3 mM.

When the enzyme electrode was not in use, it was stored at 4 °C in dry condition. No obvious decrease in the response to ATCl was observed in the first 10-day storage. After a 30-day storage period, the sensor retained 90% of its initial current response. It indicated that this interface provided a biocompatible microenvironment around the enzyme to stabilize its biological activity to a large extent.

4. Conclusions

We have demonstrated in this paper the application of electrodeposited nanoparticles for facilitating electron transfer across self-assembled monolayers. The presence of AuNPs not only provided a conductive pathway to promote electron transfer reactions at a lower potential, but also increased the surface hydrophilicity for immobilization of enzyme. The immobilized AChE, as a model showed excellent activity to its substrate and could be used for quantitative measure of organophosphate pesticide. The electrodeposited AuNPs combining with the unique properties of SAMs circumvented the drawbacks of electron transfer and offered a simple method for further functionalization by biomolecules. It provided a new avenue for biosensor design.

Acknowledgements

The authors are gratefully acknowledging the financial support of the National Natural Science Foundation of China (No. 20705010) and the Natural Science Foundation of Hubei Province (No. 2006ABA183).

References

[1] W. Yoshida, K. Sode, K. Ikebukuro, Anal. Chem. 78 (2006) 3296.
[2] W.W. Yang, J.X. Wang, S. Zhao, Y.Y. Sun, C.Q. Sun, Electrochem. Commun. 8 (2006) 665.
[3] L. Qian, X.R. Yang, Talanta 68 (2006) 721.
[4] M.H. Shi, J.J. Xu, S. Zhang, B.H. Liu, J.L. Kong, Talanta 68 (2006) 1089.
[5] V.B. Kandimalla, H.X. Ju, Chem. Eur. J. 12 (2006) 1074.
[6] D. Du, S.Z. Chen, J. Cai, A.D. Zhang, Talanta 74 (2008) 766.
[7] J. Haccoun, B. Piro, V. NoÃÃl, M.C. Pham, Bioelectrochemistry 68 (2006) 218.
[8] J.C. Vidal, S. Esteban, J. Gil, J.R. Castillo, Talanta 68 (2006) 791.
[9] I. Willner, N. Lapidot, A. Riklin, R. Kasher, E. Zahavy, E. Katz, J. Am. Chem. Soc. 116 (1994) 1428.
[10] S. Lofas, B. Johnsson, Chem. Commun. (1990) 1526.
[11] P.L. Schilardi, P. Dip, P.C. dos Santos Claro, G.A. Bentez, M.H. Fonticelli, O. Azzaroni, R.C. Salvarezza, Chem. Eur. J. 12 (2006) 38.
[12] L. Wang, J.Y. Bai, P.F. Huang, H.J. Wang, L.Y. Zhang, Y.Q. Zhao, Electrochem. Commun. 8 (2006) 1825.
[13] S. Balasubramanian, A. Revzin, A. Simoniana, Electroanalyst 18 (2006) 1885.
[14] X.Q. Ding, J.B. Hu, Q.L. Li, Talanta 68 (2006) 653.
[15] M.G. Cerruti, M. Sauthier, D. Leonard, D. Liu, G. Duscher, D.L. Feldheim, S. Franzen, Anal. Chem. 78 (2006) 3282.
[16] H.J. Lee, D. Nedelkov, R.M. Corn, Anal. Chem. 78 (2006) 6504.
[17] F. Cecchet, M. Marcaccio, M. Margotti, F. Paolucci, S. Rapino, P. Rudolf, J. Phys. Chem. B 110 (2006) 2241.
[18] A.I. Abdelrahman, A.M. Mohammad, T. Okajima, T. Ohsaka, J. Phys. Chem. B 110 (2006) 2798.
[19] X. Dai, O. Nekrassova, M.E. Hyde, R.G. Compton, Anal. Chem. 76 (2004) 5924.
[20] M.C. Daniel, D. Astruc, Chem. Rev. 104 (2004) 293.
[21] L. Su, L.Q. Mao, Talanta 70 (2006) 68.
[22] K.C. Grabar, R. GrWith Freeman, M.B. Hommer, M.J. Natan, Anal. Chem. 67 (1995) 735.
[23] M.S. El-Deab, T. Okajima, T.J. Ohsaka, J. Electrochem. Soc. 150 (2003) A851.
[24] P.N. Deepa, M. Kanungo, G. Claycomb, P.M.A. Sherwood, M. Collinson, Anal. Chem. 75 (2003) 5399.
[25] E. Majid, S. Hrapovic, Y.L. Liu, K.B. Male, J.H.T. Luong, Anal. Chem. 78 (2006) 762–769.
[26] C.Z. Li, Y.L. Liu, J.H.T. Luong, Anal. Chem. 77 (2005) 478.
[27] M.O. Finot, G.D. Braybrook, M.T. McDermott, J. Electroanal. Chem. 466 (1999) 234.
[28] P. Xu, S.Y. Du, S.J. Dong, E. Wang, Anal. Chem. 77 (2005) 8166.

[29] S. Trasatti, O.A. Petrii, J. Electroanal. Chem. 327 (1992) 353.
[30] G.T. Filho, L.H. Dall, L. Antonia, G. Jerkiewiez, J. Electroanal. Chem. 422 (1997) 149.
[31] C.J. Zhong, M.D. Porter, J. Am. Chem. Soc. 116 (1994) 11616.
[32] M.M. Walczak, D.D. Popenoe, R.S. Deinhammer, B.D. Lamp, C. Chung, M.D. Porter, Langmuir 7 (1991) 2687.
[33] T. Sumi, K. Uosaki, J. Phys. Chem. B 108 (2004) 6422.
[34] L.H. Dubois, B.R. Zegarski, J. Chem. Phys. 98 (1993) 678.
[35] N. Patel, M.C. Davies, M. Hartshorne, R.J. Heaton, C.J. Roberts, S.J.B. Tendler, P.M. Williams, Langmuir 13 (1997) 6485.
[36] H. Schulze, S. Vorlová, F. Villatte, T.T. Bachmann, R.D. Schmid, Biosens. Bioelectron. 18 (2003) 201.
[37] G.D. Liu, S.L. Riechers, M.C. Mellen, Y.H. Lin, Electrochem. Commun. 7 (2005) 1163.